



Published in final edited form as:

*Invest Ophthalmol Vis Sci.* 2008 September ; 49(9): 3821–3829. doi:10.1167/iovs.07-1470.

## Accelerated Accumulation of Lipofuscin Pigments in the RPE of a Mouse Model for *ABCA4*-Mediated Retinal Dystrophies following Vitamin A Supplementation

Roxana A. Radu<sup>1</sup>, Quan Yuan<sup>1</sup>, Jane Hu<sup>1</sup>, Jennifer H. Peng<sup>1</sup>, Marcia Lloyd<sup>1</sup>, Steven Nusinowitz<sup>1</sup>, Dean Bok<sup>1,2,3</sup>, and Gabriel H. Travis<sup>1,3,4</sup>

<sup>1</sup> Department of Ophthalmology, University of California at Los Angeles School of Medicine, Los Angeles, California

<sup>2</sup> Department of Neurobiology, University of California at Los Angeles School of Medicine, Los Angeles, California

<sup>3</sup> Brain Research Institute, University of California at Los Angeles School of Medicine, Los Angeles, California

<sup>4</sup> Department of Biological Chemistry, University of California at Los Angeles School of Medicine, Los Angeles, California

### Abstract

**Purpose**—Dietary supplementation with vitamin A is sometimes prescribed as a treatment for retinitis pigmentosa, a group of inherited retinal degenerations that cause progressive blindness. Loss-of-function mutations in the *ABCA4* gene are responsible for a subset of recessive retinitis pigmentosa. Other mutant alleles of *ABCA4* cause the related diseases, recessive cone-rod dystrophy, and recessive Stargardt macular degeneration. Mice with a knockout mutation in the *abca4* gene massively accumulate toxic lipofuscin pigments in the retinal pigment epithelium. Treatment of these mice with fenretinide, an inhibitor of vitamin A delivery to the eye, blocks formation of these toxic pigments. Here the authors tested the hypothesis that dietary supplementation with vitamin A may accelerate lipofuscin pigment formation in *abca4*<sup>-/-</sup> mice.

**Methods**—Wild-type and *abca4*<sup>-/-</sup> mice were fed normal or vitamin A-supplemented diets. Tissues from these mice were analyzed biochemically for retinoids and lipofuscin pigments. Eyes from these mice were analyzed morphologically for lipofuscin in the retinal pigment epithelium and for degeneration of photoreceptors. Visual function in these mice was analyzed by electroretinography.

**Results**—Mice that received vitamin A supplementation had dramatically higher levels of retinyl esters in the liver and retinal pigment epithelium. Lipofuscin pigments were significantly increased by biochemical and morphologic analysis in wild-type and *abca4*<sup>-/-</sup> mice fed the vitamin A-supplemented diet. Photoreceptor degeneration was observed in 11-month-old albino, but not pigmented, *abca4*<sup>-/-</sup> mice on both diets.

---

Corresponding author: Gabriel H. Travis, Department of Ophthalmology, Jules Stein Eye Institute, 100 Stein Plaza, University of California at Los Angeles School of Medicine, Los Angeles, CA 90095; travis@jsei.ucla.edu.

Disclosure: **R.A. Radu**, None; **Q. Yuan**, None; **J. Hu**, None; **J.H. Peng**, None; **M. Lloyd**, None; **S. Nusinowitz**, None; **D. Bok**, None; **G.H. Travis**, None

**Conclusions**—Vitamin A supplementation should be avoided in patients with *ABCA4* mutations or other retinal or macular dystrophies associated with lipofuscin accumulation in the retinal pigment epithelium.

Retinitis pigmentosa (RP) is an inherited blinding disease caused by the degeneration of rod and cone photoreceptor cells. The prevalence of RP in the general population is approximately 1 in 4000.<sup>1</sup> Rods in the peripheral retina are affected first, leading to the early RP symptoms of tunnel vision and night blindness. Involvement of cones and central retinal degeneration occur later in the disease course. In a randomized clinical trial, RP patients who received oral vitamin A supplementation showed slower declines in the cone response by electroretinography (ERG) than patients who received either vitamin E or no vitamin supplementation.<sup>2</sup> The beneficial effect of vitamin A on the ERG in these patients was small and not accompanied by preservation of visual acuity or visual fields. Nonetheless, given the absence of treatment alternatives, many physicians prescribe supplemental vitamin A to their RP patients based on the results of this trial.

RP, which can be transmitted as an autosomal dominant, autosomal recessive, or X-linked trait, is caused by mutations in any of 45 distinct genetic loci.<sup>3</sup> These RP genes encode proteins that perform a wide range of cellular processes including signal transduction, regeneration of visual chromophore, protein trafficking, RNA splicing, and maintenance of photoreceptor structure. One gene affected in RP is *ABCA4* (also *ABCR*). Mutations in *ABCA4* account for approximately 3% of autosomal recessive RP.<sup>4</sup> Mutations in *ABCA4* can also cause the related diseases, recessive cone-rod dystrophy and recessive Stargardt macular degeneration.<sup>4–6</sup> The *ABCA4* gene encodes an ATP-binding cassette transporter in the rims of rod and cone outer segment (OS) discs.<sup>7–9</sup> The *Abca4* transporter appears to function as a flippase for the Schiff-base conjugate of all-*trans*-retinaldehyde (all-*trans*-RAL) and phosphatidylethanolamine, called *N*-retinylidene-phosphatidylethanolamine (*N*-ret-PE).<sup>10–13</sup> *Abca4*, therefore, helps to clear all-*trans*-RAL released by rhodopsin and cone-opsin photopigments after light exposure. Removal of all-*trans*-RAL from OS discs is required for the recovery of light sensitivity after a photobleach because all-*trans*-RAL recombines noncovalently with apo-opsin to form a “noisy” photoproduct that activates transducin.<sup>14,15</sup> Consistent with these observations, Stargardt patients and *abca4*<sup>-/-</sup> mice exhibit delayed recovery of rod sensitivity after exposure to light (delayed dark adaptation).<sup>10,16</sup>

A feature of *ABCA4*-mediated retinal and macular dystrophies is the accumulation of autofluorescent lipofuscin pigments in cells of the retinal pigment epithelium (RPE).<sup>17,18</sup> This accumulation is responsible for the characteristic dark choroid seen in Stargardt patients during fluorescein angiography.<sup>19</sup> A major fluorophore of lipofuscin is the *bis*-retinoid pyridinium salt A2E.<sup>20</sup> A2E has been shown to be cytotoxic in multiple studies. For example, A2E sensitizes RPE cells to blue-light damage,<sup>21–23</sup> impairs the degradation of phospholipids in phagocytosed OS fragments,<sup>24</sup> induces the release of proapoptotic proteins from mitochondria,<sup>25,26</sup> and destabilizes cellular membranes through its properties as a cationic detergent.<sup>27–29</sup> A2E is oxidized *in vivo* by singlet oxygen in the presence of light to yield a series of oxiranes or epoxides.<sup>30,31</sup> A2E epoxides were shown to induce DNA fragmentation by forming adducts with purines and pyrimidines in cultured ARPE-19 cells,<sup>32</sup> representing still another mechanism of A2E cytotoxicity. Degeneration of photoreceptors in the *ABCA4*-mediated retinal and macular dystrophies probably begins with A2E poisoning of the RPE.

Given that all-*trans*-RAL is a primary reactant in the biogenesis of A2E, we previously tested the therapeutic strategy of slowing rhodopsin regeneration to reduce light-dependent formation of all-*trans*-RAL and thereby inhibit A2E formation. First, we used the visual-cycle inhibitor 13-*cis*-retinoic acid (Accutane; Roche, Indianapolis, IN).<sup>33–35</sup> Treatment of *abca4*<sup>-/-</sup> mice with 13-*cis*-retinoic acid (Accutane; Roche) reduced the levels of *N*-ret-PE and blocked the

accumulation of A2E and other lipofuscin pigments in the RPE.<sup>31,36</sup> A second strategy involved the use of fenretinide (4-hydroxyphenylretinamide). Fenretinide displaces all-*trans*-ROL from retinol-binding protein (RBP) in blood.<sup>37</sup> This causes mild vitamin A deficiency in the eye because the eye is critically dependent on RBP for the delivery of vitamin A.<sup>38</sup> Treatment of *abca4*<sup>-/-</sup> mice with fenretinide also potently blocked the accumulation of lipofuscin fluorophores in the RPE.<sup>39</sup> These results suggest that fenretinide may slow lipofuscin accumulation and, hence, photoreceptor degeneration in human *ABCA4*-mediated retinal dystrophies.

Given that an ocular deficiency of vitamin A was protective against lipofuscin accumulation in an animal model of *ABCA4*-mediated retinal dystrophy, it seemed possible that vitamin A supplementation could accelerate lipofuscin-accumulation in RP patients with *ABCA4* mutations. To test this possibility, we fed wild-type and *abca4*<sup>-/-</sup> mice a diet supplemented with vitamin A for several months and then measured levels of the lipofuscin fluorophores in their eyes. We observed significantly elevated levels of A2E and A2E precursors in mice receiving supplemental vitamin A.

## Materials and Methods

### Mice

Pigmented 129/Sv and albino BALB/c mouse strains on wild-type and *abca4*<sup>-/-</sup> genetic backgrounds were raised in cages under 12 hours of cyclic light (20–50 lux). Mice were fed a standard rodent diet containing 24,500 IU/kg vitamin A (NIH-31, 7013; Harlan Teklad, Madison, WI) or an otherwise identical diet containing 120,000 IU/kg vitamin A (Harlan Teklad). The vitamin A was provided as all-*trans*-retinyl palmitate (all-*trans*-RP), similar to vitamin A supplements in humans. Mice were started on the vitamin A-supplemented diet at 2 months of age. All mice studied were homozygous for the wild-type (Leu450) allele of the *rpe65* gene. Work on mice was conducted in adherence to the ARVO Statement for the Use of Animals in Ophthalmic and Vision Research.

### Preparation of Eyecups

Mice were dark adapted overnight, and all tissue manipulations were performed under dim red light (Wratten 1A filter; Eastman Kodak, Rochester, NY). After euthanatization, eyeballs were removed and hemisected. The anterior portion containing the cornea, lens, and vitreous was discarded. Eyecups, containing retina, RPE, choroid, and sclera, were frozen in liquid N<sub>2</sub> and stored at -80°C for further processing.

### Analysis of Retinoids

Single eyecups were homogenized in 1 mL phosphate-buffered saline (PBS), pH 7.2, containing 200 mM hydroxylamine. One milliliter ethanol and 3 mL hexane were added, and samples were vortexed and centrifuged at 3000g for 5 minutes. The organic phase was collected, dried under a stream of argon gas, and redissolved in 100  $\mu$ L hexane. Extracts were analyzed by normal-phase, high-performance liquid chromatography (HPLC) on a silica column (Zorbax-Sil 5  $\mu$ m, 250  $\times$  4.6 mm; Agilent Technologies, Wilmington, DE) using gradient elution (0.2%–10% dioxane in hexane) at a flow rate of 2 mL/min. The HPLC system was a liquid chromatograph (model 1100; Agilent) equipped with a photodiode-array detector. The identity of each retinoid peak was confirmed by online spectral analysis and by coelution with an authentic standard. Data were reported in picomoles per eye.

### Analysis of Lipofuscin Fluorophores by Normal-Phase Liquid Chromatography

Single eyecups were homogenized in 1 mL PBS. Four milliliters chloroform/methanol (2:1, vol/vol) was added, and the samples were extracted with the addition of 4 mL chloroform and 3 mL dH<sub>2</sub>O, followed by centrifugation at 1000g for 10 minutes. Extraction was repeated with the addition of 4 mL chloroform. Organic phases were pooled, dried under a stream of argon, and redissolved in 100  $\mu$ L 2-propanol. A2E and A2E precursors were analyzed by normal-phase HPLC with the same column and chromatograph used for retinoid analysis. The mobile phase was hexane/2-propanol/ethanol/25 mM potassium phosphate/glacial acetic acid (485:376:100:45:0.275 vol/vol) and was filtered before use. The flow rate was 1 mL/min. Column and solvent temperatures were maintained at 35°C. Absorption units at 435 nm were converted to picomoles using a calibration curve with an authentic A2E standard and the published molar extinction coefficient for A2E.<sup>40</sup>

### Identification of the 500-nm Absorbing Peak by Electrospray-Ionization Mass Spectrometry

Fifty eyecups from 3- to 6-month-old *abca4*<sup>-/-</sup> mice were homogenized in 1 mL PBS and were analyzed by normal-phase chromatography, as described. We collected the 500-nm absorbing peak fraction that eluted at 9.3 to 9.7 minutes in approximately 400  $\mu$ L. For reverse-phase chromatography, 20  $\mu$ L of this fraction was evaporated to dryness under a stream of nitrogen and redissolved in 10  $\mu$ L methanol. A portion of this sample (0.25  $\mu$ L) was separated on a capillary liquid chromatography system (model 1100; Agilent) equipped with a column (250  $\times$  0.5 mm, five  $\mu$ m; Zorbax 300SB-C18; Agilent). An isocratic solvent system of 71:5:5 (vol/vol) methanol/hexane/0.1% ammonium acetate was applied. The flow rate was 10  $\mu$ L/min. The elution profile was monitored by a diode-array detector coupled with an ion-trap mass spectrometer (LCQ Deca XP; Thermo Electron, Waltham, MA) in positive-ion mode using nitrogen as the sheath gas. The capillary temperature was 225°C, the electrospray voltage was 5.0 KeV, and the capillary voltage was 16 V. Three scan events were used, as follows: 400 to 1600 *m/z* full-scan mass spectrometry (MS); data-dependent full-scan MS/MS on the most intense ion in the full-scan spectrum; and data-dependent full-scan MS<sup>3</sup> on the most intense ion from the MS/MS full scan. The MS/MS collision energy was set to 40 V. When an *m/z* ratio for an ion was selected for a data-dependent scan, it was placed on a list and dynamically excluded from further fragmentation for 1 minute.

### Spectral Analysis of the 500-nm Absorbing Peak during Base Titration

Two hundred microliters of the normal-phase 500-nm peak fraction was evaporated to dryness under a stream of argon and redissolved in 200  $\mu$ L acetonitrile/water (75:25), transferred to a quartz cuvette, and analyzed in a spectrophotometer (UV-2400PC; Shimadzu, Kyoto, Japan). UV-visible spectra were acquired initially and after sequential addition of 1- $\mu$ L samples of 10 mN NaOH. After each addition, the sample was mixed by trituration, and the spectrum was obtained after 5-minute incubation at room temperature.

### Analysis of Retinoids in Liver

After euthanatization, mouse livers were removed, and 20 to 50 mg wet tissue was homogenized in 1 mL PBS containing 0.1% SDS. One milliliter ethanol was added, and retinoids were extracted twice with 2 mL hexane and analyzed by normal-phase HPLC as described. Data were reported as micromoles of each retinoid per gram wet weight of liver.

### Analysis of Serum Retinol

Blood was collected in capillary blood collection tubes (CapiJect; Terumo Medical, Elkton, MD) from the facial veins of mice. Serum was obtained by centrifuging the clotted blood at 1200g for 10 minutes. Retinol was extracted from the serum by the addition of 500  $\mu$ L PBS containing 0.1% SDS, 500  $\mu$ L ethanol, and 2 mL hexane. The organic phase was collected and

processed as described. Data were normalized to the volume of serum and reported as picomoles per microliter.

### Confocal Microscopy

Mice were euthanatized under anesthesia, their eyes were removed, anterior segments were dissected away, and eyecups were fixed overnight at 4°C in 0.1% PBS and 4% paraformaldehyde. Eyecups were infiltrated with 10% sucrose in PBS for 1 hour and 20% sucrose in PBS for 2 hours and then embedded in OCT compound (Sakura, Torrance, CA). Ten-micrometer cryostat sections were cut and mounted on slides (Superfrost Plus; Erie Scientific, Portsmouth, NH). Sections were warmed to room temperature, and coverslips were mounted with 5% n-propyl gallate in 100% glycerol mounting medium. Images of the mouse retina sections were captured with a confocal microscope (LSM 510; Carl Zeiss, Oberkochen, Germany) under a 63× oil objective using an excitation wavelength of 488 nm and an emission wavelength of 505 to 530 nm.

### Light and Electron Microscopy

Mice were euthanatized under anesthesia and fixed by vascular perfusion with 2% formaldehyde and 2.5% glutaraldehyde in 0.2 M sodium phosphate buffer, pH 7.2. Eyecups were divided into nasal and temporal hemispheres and fixed additionally in 1% osmium tetroxide with 0.2 M sodium phosphate, then dehydrated in a graded series of alcohols. Temporal hemispheres were embedded in an epon/araldite mixture (5 parts/3 parts) for light microscopy. Nasal hemispheres were cut into quadrants and embedded (Araldite 502; Ted Pella, Redding, CA) for electron microscopy. Sections for light microscopy were cut at 1 μm and stained with 1% toluidine blue and 1% sodium borate. These sections were photographed with a light microscope under a 40× oil objective (Axioplan; Carl Zeiss Meditec, Dublin, CA) equipped with a digital camera (CoolSNAP; Roper Scientific, Duluth, GA). All light micrographic images were obtained from temporal hemisphere sections of the retina at a distance of a single 40× field inferior to the optic nerve. Ultrathin sections for electron microscopy were cut on an ultramicrotome (Ultracut; Leica, Wetzlar, Germany). The sections were collected on 200-mesh copper grids and stained with uranium and lead salts before viewing with an electron microscope (910; Carl Zeiss). Electron microscopic images were acquired from sections of the inferior nasal quadrant.

### Quantitation of Lipofuscin Pigment Granules

Ten fields of RPE cells from each group of mice were photographed at a constant magnification using a digital camera (KeenView; Olympus, Tokyo, Japan). The total lipofuscin area was compared with the total pigment epithelium cytoplasm area from each field. Each field was considered as  $n = 1$ . SPSS software (Analysis; SPSS, Chicago, IL) was used to outline the specific areas of interest. Results were presented as mean ± SD, and statistical analysis was performed using the Student's *t*-test.

### Electroretinography

After overnight dark adaptation, mice were anesthetized by intraperitoneal injection of ketamine (150 mg/kg body weight) and xylazine (3.0 mg/kg body weight). ERGs were recorded from the corneal surface of the right eye after pupil dilation (with 1 drop of 1% atropine sulfate) using a gold loop corneal electrode with mouth-reference and tail-ground electrodes, as previously described.<sup>41</sup> One drop of methyl-cellulose (2.5%), placed on the corneal surface, ensured electrical contact and corneal integrity. Responses were amplified (CP511 AC amplifier, 10,000×; 3 dB down at 2 and 10,000 Hz; Grass Instruments, Quincy, MA) and digitized on a personal computer using an I/O board (PCI-1200; National Instruments, Austin, TX). Signal processing was performed with custom software (LabWindows/CVI; National



Instruments). Mouse body temperature was maintained at 38°C with a heated water pad. All stimuli were presented in a large Ganzfeld dome (LKC Technologies, Gaithersburg, MD).

Dark-adapted ERGs were recorded to blue (Wratten 47A or 47B; Eastman Kodak) light flashes up to a maximum intensity of 1.51 log cd · s/m<sup>2</sup> measured at the corneal surface. At the highest intensities, the rod-mediated *a*-wave of the ERG was clearly saturated. The leading edge of the *a*-wave was fitted with a computational model to provide estimates of photoreceptor activity.<sup>42,43</sup> The model generated estimates for *S*, a sensitivity (or gain) parameter, and *R<sub>mp3</sub>*, the maximum saturated photoreceptor photovoltage. Peak-to-peak amplitudes measured from responses over the range −3.64 to 0.7 log cd · s/m<sup>2</sup> were fitted with a Naka-Rushton function to derive estimates for *V<sub>max</sub>*, the *b*-wave-saturated amplitude, and *k*, response sensitivity. The kinetics of rod photoreceptor recovery from a photobleach was studied by exposing mice to 1000 lux white light for 1 minute in a Ganzfeld dome,<sup>41</sup> which bleached approximately 60% of the rhodopsin. After the mouse was returned to darkness, the time course of rod recovery was examined by monitoring the growth of the rod ERG *b*-wave to a dim blue probe-flash (−0.54 log cd · s/m<sup>2</sup>). ERGs were recorded at 1-minute intervals for 30 minutes. Flash sequence and presentation frequency were controlled by computer. Finally, cone-mediated responses were recorded to white flashes (−0.58 to 0.638 log cd · s/m<sup>2</sup>) after 10 minutes of adaptation to a rod-saturating background (32 cd/m<sup>2</sup>).

## Results

### Retinoid Levels in Control and Vitamin A–Supplemented Mice

Serum levels of all-*trans*-ROL were similar in *abca4*<sup>−/−</sup> mice fed the normal and vitamin A–supplemented diets for the first 3 months (Fig. 1A). After 4 months, vitamin A–supplemented mice had higher levels of serum all-*trans*-ROL. Hepatic all-*trans*-RE accumulated more rapidly in *abca4*<sup>−/−</sup> mice receiving supplemental vitamin A (Fig. 1B). Levels of all-*trans*-RE in *abca4*<sup>−/−</sup> eyecups also increased dramatically with vitamin A supplementation (Fig. 1C). In contrast, we observed no difference in the levels of 11-*cis*-retinaldehyde (11-*cis*-RAL) visual chromophore (Fig. 1D). Representative chromatograms of retinoids from control and vitamin A–supplemented mouse eye-cups are shown in Figures 1E and 1F. We observed similar effects on the levels of retinoids in wild-type mice receiving vitamin A supplementation (not shown).

### Identification of A2PE-H<sub>2</sub> in Eyecup Homogenates from *abca4*<sup>−/−</sup> Mice

A2E, the major fluorophore of lipofuscin in RPE cells,<sup>20</sup> is elevated approximately 20-fold in *abca4*<sup>−/−</sup> versus wild-type mice<sup>10</sup> (Fig. 2A). The wavelength of maximal absorbance ( $\lambda_{\max}$ ) for A2E is 434 nm<sup>20</sup> (Fig. 2A, inset). A second constituent of lipofuscin, with a  $\lambda_{\max}$  of approximately 500 nm, is 32-fold elevated in *abca4*<sup>−/−</sup> versus wild-type eyecups<sup>11</sup> (Fig. 2B). We tentatively identified the molecule responsible for this 500-nm absorption as the A2E-precursor, A2PE-H<sub>2</sub>.<sup>11,44</sup> Alternatively, it has been suggested that the major 500-nm absorbing species in *abca4*<sup>−/−</sup> mouse eyes is the protonated Schiff-base conjugate of all-*trans*-RAL-dimer with ethanolamine or a phosphatidylethanolamine,<sup>45</sup> or di-hydro-A2E (A2E-H<sub>2</sub>),<sup>46</sup> which lacks the phosphatidic acid moiety of A2PE-H<sub>2</sub>. To distinguish between these possibilities, we collected the 9.5-minute, 500-nm peak fraction during normal-phase liquid chromatography of *abca4*<sup>−/−</sup> eyecup extracts (Fig. 2B) and submitted it to reverse phase chromatography and electrospray-ionization (ESI)-MS. The 500-nm absorbing material eluted in a major peak between 16.5 and 19.5 minutes (Fig. 2C). The 10-nm difference in  $\lambda_{\max}$  of the 500-nm absorbing peak between normal- and reverse-phase chromatography (Figs. 2B, 2C, insets) is a solvent effect of the two mobile phases. ESI-MS analysis showed that this 500-nm peak coeluted with a dominant, singly charged ion of *m/z* 1014.81 (Figs. 2D, 2E). The mass of this major ion within the 500-nm peak fraction corresponded to the mass of mono-stearoyl-A2PE-H<sub>2</sub> (1014.73 amu) (Fig. 2G) and the mono-stearoyl-phosphatidylethanolamine Schiff-base of

all-*trans*-RAL-dimer, but not to A2E-H<sub>2</sub> (594.5 amu). Collision-induced fragmentation of this parent ion yielded no additional structural information. To distinguish between A2PE-H<sub>2</sub> and all-*trans*-RAL-dimer protonated Schiff-base, we performed UV-spectral analysis during NaOH-titration of the 9.5-minute normal-phase peak fraction (Fig. 2B). If a protonated Schiff-base were responsible for the 500-nm absorption, the addition of NaOH in molar excess would deprotonate it, causing a significant hypsochromic shift in the spectrum. We observed no detectable reduction of 500-nm absorbance during base titration (Fig. 2F) despite the addition of an estimated 20-fold molar excess of NaOH. These results suggest that the 500-nm absorbing compound, which is dramatically elevated in *abca4*<sup>-/-</sup> eyecups (Fig. 2B) and postmortem RPE samples from patients with Stargardt disease,<sup>11</sup> is mono-stearyl A2PE-H<sub>2</sub> or its open-ring precursor, mono-stearyl-PE-*bis*-all-*trans*-RAL Schiff-base (Fig. 2G).

### Increased Lipofuscin Fluorophores in Mice Receiving Supplemental Vitamin A

We measured levels of A2PE-H<sub>2</sub> and A2E in eyecup extracts from *abca4*<sup>-/-</sup> mice fed control and vitamin A-supplemented diets. In mice from both groups, the levels of these compounds increased with advancing age (Figs. 3A, 3B). In fact, we observed significantly higher levels of A2PE-H<sub>2</sub> and A2E in mice receiving the vitamin A-supplemented diet at several ages (Figs. 3A, 3B).

To confirm these results, we analyzed the content of lipofuscin pigments in the RPE of control-fed and vitamin A-supplemented albino mice by two approaches. Laser confocal microscopy of retina sections showed higher autofluorescence in the RPE from *abca4*<sup>-/-</sup> compared with wild-type (BALB/c) mice fed a normal diet (Figs. 4A, 4B). Autofluorescence in the RPE comes mainly from lipofuscin.<sup>47</sup> Autofluorescence was still higher in vitamin A-supplemented *abca4*<sup>-/-</sup> mice (Fig. 4C), consistent with the higher A2E in these animals (Fig. 3B). Electron microscopic analysis of retinal sections from the fellow eye showed more lipofuscin pigment granules in *abca4*<sup>-/-</sup> than in wild-type (Figs. 4D, 4E) RPE from mice fed the control diet and still more granules in RPE from *abca4*<sup>-/-</sup> mice fed the vitamin A-supplemented diet (Fig. 4F). To quantify these lipofuscin pigments, we measured the areas within RPE cells occupied with pigment granules divided by the total cytoplasmic areas. The determined fractional areas of lipofuscin granules in the RPE are shown below each electron micrograph in Figures 4D, 4E, and 4F.

We also measured levels of A2PE-H<sub>2</sub> and A2E in 6-month-old wild-type mice (strain 129/Sv) after 4 months of vitamin A supplementation. Although the absolute levels were lower in wild-type than in *abca4*<sup>-/-</sup> mice, we observed higher levels of these pigments in the vitamin A-supplemented compared with the control-fed mice (Fig. 5).

### Histologic Analysis

Previously, we observed no significant photoreceptor degeneration in 6-month-old pigmented *abca4*<sup>-/-</sup> mice.<sup>48</sup> In the present study, we examined retinas from 11-month-old albino wild-type and *abca4*<sup>-/-</sup> mice by light microscopy. Retinas from wild-type albino mice fed the control diet contained 10 to 11 rows of nuclei in the outer nuclear layer (ONL; Fig. 6A). In contrast, retinas from *abca4*<sup>-/-</sup> mice fed both diets contained six to seven rows (Figs. 6B, 6C). The OS layer was also thinner in albino *abcr*<sup>-/-</sup> than in wild-type (Fig. 6) mice. Therefore, by 11 months, photoreceptors were approximately 40% degenerate with OS shortening in albino *abca4*<sup>-/-</sup> mice irrespective of diet.

### Electroretinographic Analysis of Control-Fed and Vitamin A-Supplemented Pigmented *abca4*<sup>-/-</sup> Mice

We performed ERG analysis on age-matched wild-type and *abca4*<sup>-/-</sup> mice fed the control and vitamin A-supplemented diets. No significant differences were observed in rod-mediated *a*-

wave parameters ( $S$  and  $RmP_3$ ) or  $b$ -wave parameters ( $V_{\max}$  and  $k$ ) among these four sets of mice (not shown). Similarly, we observed no significant differences attributable to diet among cone-mediated  $b$ -wave amplitudes in wild-type (Fig. 7A) or  $abca4^{-/-}$  (Fig. 7B) mice. We did observe a trend toward faster recovery of rod sensitivity after a photobleach at the later time points in vitamin A-fed mice (Fig. 7C). However, at most times during recovery, this trend did not reach statistical significance.

## Discussion

The prescribed dose of vitamin A for RP patients is 15,000 IU/d all-*trans*-RP,<sup>2</sup> five times the reference dose of 3000 IU/d for adult humans.<sup>49</sup> To duplicate this degree of supplementation in mice, we prepared a rodent diet containing 120,000 IU/kg all-*trans*-RP, five times the reference content of 24,000 IU/kg in the standard rodent diet.<sup>50</sup> Although serum levels of all-*trans*-ROL increased only modestly in vitamin A-supplemented mice (Fig. 1A), all-*trans*-RE in the liver (Fig. 1B) and eyecups (Fig. 1C) was significantly elevated. Levels of 11-*cis*-RAL, however, did not change (Fig. 1D). Nearly all the 11-*cis*-RAL in a dark-adapted vertebrate eye is bound to rhodopsin. Nonexpansion of the 11-*cis*-RAL pool despite higher total retinoids suggested that dietary supplementation did not increase the content of rhodopsin in the mice.

Mice and humans with loss-of-function mutations in the *ABCA4* gene undergo dramatic elevations of a 500-nm absorbing molecular species.<sup>11</sup> The identity of this species has been controversial. We originally suggested that it represents a phospholipid dihydro-precursor of A2E (A2PE-H<sub>2</sub>).<sup>11,44</sup> Conversion of A2PE-H<sub>2</sub> to A2E involves hydrolysis of the phospholipid to yield dihydro-A2E (A2E-H<sub>2</sub>) and subsequent oxidation to yield A2E. Consistently, incubation of the 500-nm peak fraction from  $abca4^{-/-}$  RPE under mildly acidic and oxidizing conditions resulted in the spontaneous formation of A2E.<sup>11</sup> However, two other 500-nm-absorbing compounds have been identified in  $abca4^{-/-}$  mouse eyes, A2E-H<sub>2</sub><sup>46</sup> and all-*trans*-RAL-dimer protonated Schiff-base.<sup>45,51</sup> To determine the dominant 500-nm-absorbing species in  $abca4^{-/-}$  eyecups, we used ESI-MS to analyze the 500-nm peak fraction after normal-phase chromatography. We observed a striking overlap between the reverse-phase elution profiles of the 500-nm-absorbing species and a positive ion of 1014.81  $m/z$  (Figs. 2C, 2D). This ion was virtually homogeneous during the elution period of 16.37 to 19.36 minutes (Fig. 2E). It is, therefore, likely that this 1014.81- $m/z$  ion was identical with, or a derivative of, the dominant 500-nm absorbing species in  $abca4^{-/-}$  and Stargardt eyes. The mass of this ion (1014.81) corresponded to the molecular mass of mono-stearoyl-A2PE-H<sub>2</sub> (1014.73) or the mono-stearoyl-phosphatidylethanolamine Schiff base of all-*trans*-RAL dimer but not to that of A2E-H<sub>2</sub> (594.5).

To distinguish between A2PE-H<sub>2</sub> and all-*trans*-RAL dimer-protonated Schiff base as the source of 500-nm absorption, we acquired UV-visible spectra during titration with the base. We observed no change in the absorption spectrum despite the addition of NaOH in approximately 20-fold molar excess. If the 500-nm absorption were caused by the presence of a protonated Schiff base of all-*trans*-RAL dimer, the spectrum would have changed with the disappearance of 500-nm absorbance and the appearance of new absorbance centered at 432 nm.<sup>51</sup> These results exclude all-*trans*-RAL dimer as the major 500-nm-absorbing species that accumulates in  $abca4^{-/-}$  and Stargardt eyes. A2PE-H<sub>2</sub> forms by electrocyclization after condensation of *N*-ret-PE with all-*trans*-RAL to yield the mono-stearoyl-phosphatidylethanolamine-*bis*-all-*trans*-RAL Schiff base (Fig. 2G). This electrocyclization is reversible; hence, both the closed- and the open-ring structures are likely present in ocular tissues. The open-ring isomer may be the major form in vivo because the electrocyclization reaction is probably slower than oxidation of A2PE-H<sub>2</sub> to A2PE. In addition, the open-ring isomer contains a longer resonance structure than A2PE-H<sub>2</sub>, more consistent with a  $\lambda_{\max}$  of



500 nm. It is unclear whether A2PE-H<sub>2</sub> was present in vivo as a monoacylated species or whether one of the two fatty-acyl chains was lost during tissue processing.

Dietary supplementation with vitamin A significantly increased the content of A2E and A2PE-H<sub>2</sub> after 2 months of treatment (Figs. 3A, 3B). We also consistently observed increased lipofuscin pigments in the RPE of vitamin A-supplemented compared with control-fed *abca4*<sup>-/-</sup> mice (Figs. 4B, 4C, 4E, 4F). A possible explanation for these increased lipofuscin fluorophores is that vitamin A-supplemented mice regenerate visual chromophore at a faster rate because of the increased all-*trans*-RE (Fig. 1C), which is a substrate for the isomerase. This effect would only come into play at high intensities of light, when the rate of photoisomerization exceeds the maximum turnover of the visual cycle. Supplementation with vitamin A would, therefore, yield higher levels of photoreceptor all-*trans*-RAL, which is the primary reactant in the biogenesis of A2E. A subset of recessive RP in humans is caused by loss-of-function mutations in the *ABCA4* gene.<sup>52</sup> Hence, the *abca4*<sup>-/-</sup> mouse is a good animal model for *ABCA4*-mediated retinal dystrophies. It is likely that patients with RP caused by *ABCA4* mutations who receive vitamin A supplementation would experience accelerated deposition of lipofuscin pigments.

We also observed higher levels of A2PE-H<sub>2</sub> and A2E in wild-type mice on the vitamin A-supplemented diet, though the absolute levels of these pigments were lower than in *abca4*<sup>-/-</sup> mice (Fig. 5). These results show that the effects of vitamin A supplementation on lipofuscin fluorophores are independent of the genotype at *ABCA4*. Given the low levels of these fluorophores in vitamin A-supplemented wild-type mice, it is unlikely that 15,000 IU/d vitamin A would have deleterious effects in healthy humans. The accumulation of lipofuscin pigments in the RPE is not limited to diseases caused by mutations in the *ABCA4* gene. Increased fundus autofluorescence by scanning laser ophthalmoscopy is commonly seen in patients with age-related macular degeneration.<sup>53-55</sup> This autofluorescent material has spectral properties similar to those of A2PE-H<sub>2</sub> in *abca4*<sup>-/-</sup> mice.<sup>11,56</sup> Strong fundus autofluorescence is also seen in patients with Best vitelliform macular dystrophy and a subset of patients with cone-rod dystrophy.<sup>57</sup> Vitamin A supplementation in these and other retinal or macular dystrophies associated with lipofuscin accumulation would likely accelerate the formation of lipofuscin pigments.

The randomized clinical trial of vitamin A supplementation published by Berson et al.<sup>2</sup> studied RP patients without regard to genetic etiologies that were unknown at the time. Visual function, determined by ERG analysis, was not significantly different in pigmented wild-type or *abca4*<sup>-/-</sup> mice receiving the vitamin A-supplemented diet compared with the control diet (Figs. 7A, 7B). Vitamin A supplementation increases all-*trans*-RE in the RPE (Fig. 1C), substrates for the retinoid isomerase (Rpe65) that regenerates visual chromophore.<sup>58</sup> Faster regeneration of visual chromophore after light exposure may explain the trend toward faster recovery of rod sensitivity (Fig. 7C). The ERG benefit observed in RP patients receiving supplemental vitamin A might have resulted from this faster regeneration of visual chromophore rather than from a slowing of photoreceptor degeneration, as originally suggested.<sup>2</sup>

Albino *abca4*<sup>-/-</sup> mice lost approximately 40% of photoreceptors by 11 months (Fig. 6). In contrast, pigmented *abca4*<sup>-/-</sup> mice showed no photoreceptor degeneration (Radu RA, Bok D, unpublished observations, 2008). We also observed significant thinning of the OS layer in albino *abcr*<sup>-/-</sup> mice (Fig. 6). Previously, we showed that albino *abca4*<sup>-/-</sup> mice have higher A2E-oxirane levels than pigmented *abca4*<sup>-/-</sup> mice of similar ages and light-exposure histories.<sup>31</sup> Faster photoreceptor degeneration in albino *abca4*<sup>-/-</sup> mice may be attributed to the toxic effects of A2E oxiranes in the RPE.<sup>32</sup> However, the rates of photoreceptor degeneration in control-fed and vitamin A-supplemented *abca4*<sup>-/-</sup> mice were similar (Figs. 6B, 6C). Does this imply that accelerated lipofuscin accumulation is benign? Probably not. Humans with

*ABCA4* mutations undergo photoreceptor degeneration despite the absence of photoreceptor degeneration in pigmented *abca4*<sup>-/-</sup> mice. A likely explanation is the large difference in the time frames of disease progression. Mice were studied over a period of months; in humans, RP develops over decades. Given the established cytotoxicity of A2E,<sup>21–29</sup> increasing the burden of A2E in RPE cells is likely to hasten photoreceptor degeneration.

In summary, excess dietary vitamin A promotes the accumulation of toxic lipofuscin fluorophores such as A2E in the RPE. A2E accumulation is critical to the pathogenesis in several retinal and macular diseases, including those caused by *ABCA4* mutations. Based on previous studies with *abca4*<sup>-/-</sup> mice,<sup>31,36,39</sup> progression of these diseases may be slowed by treatment with visual cycle inhibitors or vitamin A antagonists. The results presented here suggest that RP patients should be screened genetically to rule out mutations in the *ABCA4* gene before vitamin A supplements are prescribed.

## Acknowledgments

Supported by grants from the Foundation Fighting Blindness, the National Eye Institute, and the Macula Vision Research Foundation. DB is the UCLA Dolly Green Professor of Ophthalmology. GHT is the UCLA Charles Kenneth Feldman Professor and the Jules and Doris Stein Research to Prevent Blindness Professor.

## References

1. Bunker CH, Berson EL, Bromley WC, Hayes RP, Roderick TH. Prevalence of retinitis pigmentosa in Maine. *Am J Ophthalmol* 1984;97:357–365. [PubMed: 6702974]
2. Berson EL, Rosner B, Sandberg MA, et al. A randomized trial of vitamin A and vitamin E supplementation for retinitis pigmentosa. *Arch Ophthalmol* 1993;111:761–772. [PubMed: 8512476]
3. Hartong DT, Berson EL, Dryja TP. Retinitis pigmentosa. *Lancet* 2006;368:1795–1809. [PubMed: 17113430]
4. Klevering BJ, Yzer S, Rohrschneider K, et al. Microarray-based mutation analysis of the *ABCA4* (*ABCR*) gene in autosomal recessive cone-rod dystrophy and retinitis pigmentosa. *Eur J Hum Genet* 2004;12:1024–1032. [PubMed: 15494742]
5. Allikmets R, Singh N, Sun H, et al. A photoreceptor cell-specific ATP-binding transporter gene (*ABCR*) is mutated in recessive Stargardt macular dystrophy. *Nat Genet* 1997;15:236–246. [PubMed: 9054934]
6. Stone EM, Webster AR, Vandenberg K, et al. Allelic variation in *Abcr* associated with Stargardt-disease but not age-related macular degeneration. *Nat Genet* 1998;20:328–329. [PubMed: 9843201]
7. Sun H, Nathans J. Stargardt's *ABCR* is localized to the disc membrane of retinal rod outer segments. *Nat Genet* 1997;17:15–16. [PubMed: 9288089]
8. Azarian SM, Travis GH. The photoreceptor rim protein is an ABC transporter encoded by the gene for recessive Stargardt's-disease (*ABCR*). *FEBS Lett* 1997;409:247–252. [PubMed: 9202155]
9. Illing M, Molday LL, Molday RS. The 220-kDa rim protein of retinal rod outer segments is a member of the ABC transporter superfamily. *J Biol Chem* 1997;272:10303–10310. [PubMed: 9092582]
10. Weng J, Mata NL, Azarian SM, Tzekov RT, Birch DG, Travis GH. Insights into the function of Rim protein in photoreceptors and etiology of Stargardt's disease from the phenotype in *abcr* knockout mice. *Cell* 1999;98:13–23. [PubMed: 10412977]
11. Mata NL, Weng J, Travis GH. Biosynthesis of a major lipofuscin fluorophore in mice and humans with *ABCR*-mediated retinal and macular degeneration. *Proc Natl Acad Sci U S A* 2000;97:7154–7159. [PubMed: 10852960]
12. Sun H, Molday RS, Nathans J. Retinol stimulates ATP hydrolysis by purified and reconstituted *ABCR*, the photoreceptor-specific ATP-binding cassette transporter responsible for Stargardt disease. *J Biol Chem* 1999;274:8269–8281. [PubMed: 10075733]
13. Beharry S, Zhong M, Molday RS. N-retinylidene-phosphatidylethanolamine is the preferred retinoid substrate for the photoreceptor-specific ABC transporter *ABCA4* (*ABCR*). *J Biol Chem* 2004;279:53972–53979. [PubMed: 15471866]

14. Jager S, Palczewski K, Hofmann KP. Opsin/all-trans-retinal complex activates transducin by different mechanisms than photolyzed rhodopsin. *Biochemistry* 1996;35:2901–2908. [PubMed: 8608127]
15. Bartl FJ, Fritze O, Ritter E, et al. Partial agonism in a G protein-coupled receptor: role of the retinal ring structure in rhodopsin activation. *J Biol Chem* 2005;280:34259–34267. [PubMed: 16027155]
16. Fishman GA, Farbman JS, Alexander KR. Delayed rod dark adaptation in patients with Stargardt's disease. *Ophthalmology* 1991;98:957–962. [PubMed: 1866151]
17. Eagle RC Jr, Lucier AC, Bernardino VB Jr, Yanoff M. Retinal pigment epithelial abnormalities in fundus flavimaculatus: a light and electron microscopic study. *Ophthalmology* 1980;87:1189–1200. [PubMed: 6165950]
18. Birnbach CD, Jarvelainen M, Possin DE, Milam AH. Histopathology and immunocytochemistry of the neurosensory retina in fundus flavimaculatus. *Ophthalmology* 1994;101:1211–1219. [PubMed: 8035984]
19. Schwoerer J, Secretan M, Zografos L, Piguat B. Indocyanine green angiography in Fundus flavimaculatus. *Ophthalmologica* 2000;214:240–245. [PubMed: 10859505]
20. Reinboth JJ, Gautschi K, Munz K, Eldred GE, Reme CE. Lipofuscin in the retina: quantitative assay for an unprecedented autofluorescent compound (pyridinium bis-retinoid, A2-E) of ocular age pigment. *Exp Eye Res* 1997;65:639–643. [PubMed: 9367643]
21. Cubeddu R, Taroni P, Hu DN, Sakai N, Nakanishi K, Roberts JE. Photophysical studies of A2-E, putative precursor of lipofuscin, in human retinal pigment epithelial cells. *Photochem Photobiol* 1999;70:172–175. [PubMed: 10461456]
22. Sparrow JR, Nakanishi K, Parish CA. The lipofuscin fluorophore A2E mediates blue light-induced damage to retinal pigmented epithelial cells. *Invest Ophthalmol Vis Sci* 2000;41:1981–1989. [PubMed: 10845625]
23. Schutt F, Davies S, Kopitz J, Holz FG, Boulton ME. Photodamage to human RPE cells by A2-E, a retinoid component of lipofuscin. *Invest Ophthalmol Vis Sci* 2000;41:2303–2308. [PubMed: 10892877]
24. Finnemann SC, Leung LW, Rodriguez-Boulan E. The lipofuscin component A2E selectively inhibits phagolysosomal degradation of photoreceptor phospholipid by the retinal pigment epithelium. *Proc Natl Acad Sci U S A* 2002;99:3842–3847. [PubMed: 11904436]
25. Suter M, Reme C, Grimm C, et al. Age-related macular degeneration: the lipofuscin component N-retinyl-N-retinylidene ethanolamine detaches proapoptotic proteins from mitochondria and induces apoptosis in mammalian retinal pigment epithelial cells. *J Biol Chem* 2000;275:39625–39630. [PubMed: 11006290]
26. Sparrow JR, Cai B. Blue light-induced apoptosis of A2E-containing RPE: involvement of caspase-3 and protection by Bcl-2. *Invest Ophthalmol Vis Sci* 2001;42:1356–1362. [PubMed: 11328751]
27. Eldred GE, Lasky MR. Retinal age pigments generated by self-assembling lysosomotropic detergents. *Nature* 1993;361:724–726. [PubMed: 8441466]
28. Sparrow JR, Parish CA, Hashimoto M, Nakanishi K. A2E, a lipofuscin fluorophore, in human retinal pigmented epithelial cells in culture. *Invest Ophthalmol Vis Sci* 1999;40:2988–2995. [PubMed: 10549662]
29. De S, Sakmar TP. Interaction of A2E with model membranes: implications to the pathogenesis of age-related macular degeneration. *J Gen Physiol* 2002;120:147–157. [PubMed: 12149277]
30. Ben-Shabat S, Itagaki Y, Jockusch S, Sparrow JR, Turro NJ, Nakanishi K. Formation of a nonaoxirane from A2E, a lipofuscin fluorophore related to macular degeneration, and evidence of singlet oxygen involvement. *Angew Chem Int Ed Engl* 2002;41:814–817. [PubMed: 12491345]
31. Radu RA, Mata NL, Bagla A, Travis GH. Light exposure stimulates formation of A2E oxiranes in a mouse model of Stargardt's macular degeneration. *Proc Natl Acad Sci U S A* 2004;101:5928–5933. [PubMed: 15067110]
32. Sparrow JR, Vollmer-Snarr HR, Zhou J, et al. A2E-epoxides damage DNA in retinal pigment epithelial cells: vitamin E and other anti-oxidants inhibit A2E-epoxide formation. *J Biol Chem* 2003;278:18207–18213. [PubMed: 12646558]
33. Law WC, Rando RR. The molecular basis of retinoic acid induced night blindness. *Biochem Biophys Res Commun* 1989;161:825–829. [PubMed: 2660792]

34. Gamble MV, Mata NL, Tsin AT, Mertz JR, Blaner WS. Substrate specificities and 13-cis-retinoic acid inhibition of human, mouse and bovine cis-retinol dehydrogenases. *Biochim Biophys Acta* 2000;1476:3–8. [PubMed: 10606761]
35. Sieving PA, Chaudhry P, Kondo M, et al. Inhibition of the visual cycle in vivo by 13-cis retinoic acid protects from light damage and provides a mechanism for night blindness in isotretinoin therapy. *Proc Natl Acad Sci U S A* 2001;98:1835–1840. [PubMed: 11172037]
36. Radu RA, Mata NL, Nusinowitz S, Liu X, Sieving PA, Travis GH. Treatment with isotretinoin inhibits lipofuscin accumulation in a mouse model of recessive Stargardt's macular degeneration. *Proc Natl Acad Sci U S A* 2003;100:4742–4747. [PubMed: 12671074]
37. Berni R, Formelli F. In vitro interaction of fenretinide with plasma retinol-binding protein and its functional consequences. *FEBS Lett* 1992;308:43–45. [PubMed: 1386578]
38. Vogel S, Piantedosi R, O'Byrne SM, et al. Retinol-binding protein-deficient mice: biochemical basis for impaired vision. *Biochemistry* 2002;41:15360–15368. [PubMed: 12484775]
39. Radu RA, Han Y, Bui TV, et al. Reductions in serum vitamin A arrest accumulation of toxic retinal fluorophores: a potential therapy for treatment of lipofuscin-based retinal diseases. *Invest Ophthalmol Vis Sci* 2005;46:4393–4401. [PubMed: 16303925]
40. Parish CA, Hashimoto M, Nakanishi K, Dillon J, Sparrow J. Isolation and one-step preparation of A2E and iso-A2E, fluorophores from human retinal pigment epithelium. *Proc Natl Acad Sci U S A* 1998;95:14609–14613. [PubMed: 9843937]
41. Nusinowitz S, Nguyen L, Radu R, Kashani Z, Farber D, Danciger M. Electroretinographic evidence for altered phototransduction gain and slowed recovery from photobleaches in albino mice with a MET450 variant in RPE65. *Exp Eye Res* 2003;77:627–638. [PubMed: 14550405]
42. Hood DC, Birch DG. Light adaptation of human rod receptors: the leading edge of the human a-wave and models of rod receptor activity. *Vis Res* 1993;33:1605–1618. [PubMed: 8236849]
43. Hood DC, Birch DG. Rod phototransduction in retinitis pigmentosa: estimation and interpretation of parameters derived from the rod a-wave. *Invest Ophthalmol Vis Sci* 1994;35:2948–2961. [PubMed: 8206712]
44. Bui TV, Han Y, Radu RA, Travis GH, Mata NL. Characterization of native retinal fluorophores involved in biosynthesis of A2E and lipofuscin-associated retinopathies. *J Biol Chem* 2006;281:18112–18119. [PubMed: 16638746]
45. Kim SR, Jang YP, Jockusch S, Fishkin NE, Turro NJ, Sparrow JR. The all-trans-retinal dimer series of lipofuscin pigments in retinal pigment epithelial cells in a recessive Stargardt disease model. *Proc Natl Acad Sci U S A* 2007;104:19273–19278. [PubMed: 18048333]
46. Kim SR, He J, Yanase E, et al. Characterization of dihydro-A2PE: an intermediate in the A2E biosynthetic pathway. *Biochemistry* 2007;46:10122–10129. [PubMed: 17685561]
47. Delori FC, Dorey CK, Staurenghi G, Arend O, Goger DG, Weiter JJ. In vivo fluorescence of the ocular fundus exhibits retinal pigment epithelium lipofuscin characteristics. *Invest Ophthalmol Vis Sci* 1995;36:718–729. [PubMed: 7890502]
48. Mata NL, Tzekov RT, Liu XR, Weng J, Birch DG, Travis GH. Delayed dark-adaptation and lipofuscin accumulation in *abcr* +/- mice: implications for involvement of ABCR in age-related macular degeneration. *Invest Ophthalmol Vis Sci* 2001;42:1685–1690. [PubMed: 11431429]
49. Monsen ER. Dietary reference intakes for the antioxidant nutrients: vitamin C, vitamin E, selenium, and carotenoids. *J Am Diet Assoc* 2000;100:637–640. [PubMed: 10863565]
50. Council, NR. *Nutrient Requirements of Laboratory Animals*. Washington, DC: National Academy Press; 1995. Nutrient requirements of the mouse; p. 80-102.
51. Fishkin NE, Sparrow JR, Allikmets R, Nakanishi K. Isolation and characterization of a retinal pigment epithelial cell fluorophore: an all-trans-retinal dimer conjugate. *Proc Natl Acad Sci U S A* 2005;102:7091–7096. [PubMed: 15870200]
52. Klevering BJ, Deutman AF, Maugeri A, Cremers FP, Hoyng CB. The spectrum of retinal phenotypes caused by mutations in the ABCA4 gene. *Graefes Arch Clin Exp Ophthalmol* 2005;243:90–100. [PubMed: 15614537]
53. Lois N, Owens SL, Coco R, Hopkins J, Fitzke FW, Bird AC. Fundus autofluorescence in patients with age-related macular degeneration and high risk of visual loss. *Am J Ophthalmol* 2002;133:341–349. [PubMed: 11860971]

54. Einbock W, Moessner A, Schnurrbusch UE, Holz FG, Wolf S. Changes in fundus autofluorescence in patients with age-related maculopathy: correlation to visual function: a prospective study. *Graefes Arch Clin Exp Ophthalmol* 2005;243:300–305. [PubMed: 15864618]
55. Bindewald A, Bird AC, Dandekar SS, et al. Classification of fundus autofluorescence patterns in early age-related macular disease. *Invest Ophthalmol Vis Sci* 2005;46:3309–3314. [PubMed: 16123434]
56. Delori FC, Goger DG, Dorey CK. Age-related accumulation and spatial distribution of lipofuscin in RPE of normal subjects. *Invest Ophthalmol Vis Sci* 2001;42:1855–1866. [PubMed: 11431454]
57. Wabbels B, Demmler A, Paunescu K, Wegscheider E, Preising MN, Lorenz B. Fundus autofluorescence in children and teenagers with hereditary retinal diseases. *Graefes Arch Clin Exp Ophthalmol* 2006;244:36–45. [PubMed: 16034607]
58. Jin M, Li S, Moghrabi WN, Sun H, Travis GH. Rpe65 is the retinoid isomerase in bovine retinal pigment epithelium. *Cell* 2005;122:449–459. [PubMed: 16096063]



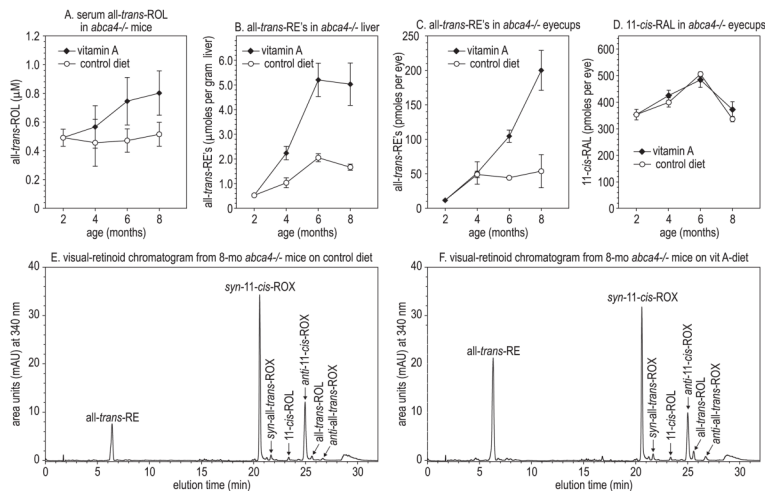


**Figure 1.** Retinoids in vitamin A-supplemented and control-fed mouse tissues. **(A)** Serum all-trans-ROL in *abca4*<sup>-/-</sup> mice, expressed in micromoles per liter at the indicated ages. **(B)** All-trans-RE in *abca4*<sup>-/-</sup> livers, expressed in micromoles per gram wet weight of tissue. **(C)** All-trans-RE in *abca4*<sup>-/-</sup> eyecups, expressed in picomoles per eye. **(D)** 11-cis-RAL in *abca4*<sup>-/-</sup> eyecups, expressed in picomoles per eye. All values are shown ± SD (*n* = 3). **(E)** Representative normal-phase chromatogram (340 nm) of retinoids from the eye of an 8-month-old *abca4*<sup>-/-</sup> mouse on the control diet. Retinaldehydes were stabilized with hydroxylamine to form their cognate oximes (ROX) before chromatography. **(F)** Representative normal-phase chromatogram of retinoids from the eye of an 8-month-old *abca4*<sup>-/-</sup> mouse on the vitamin A-supplemented diet.

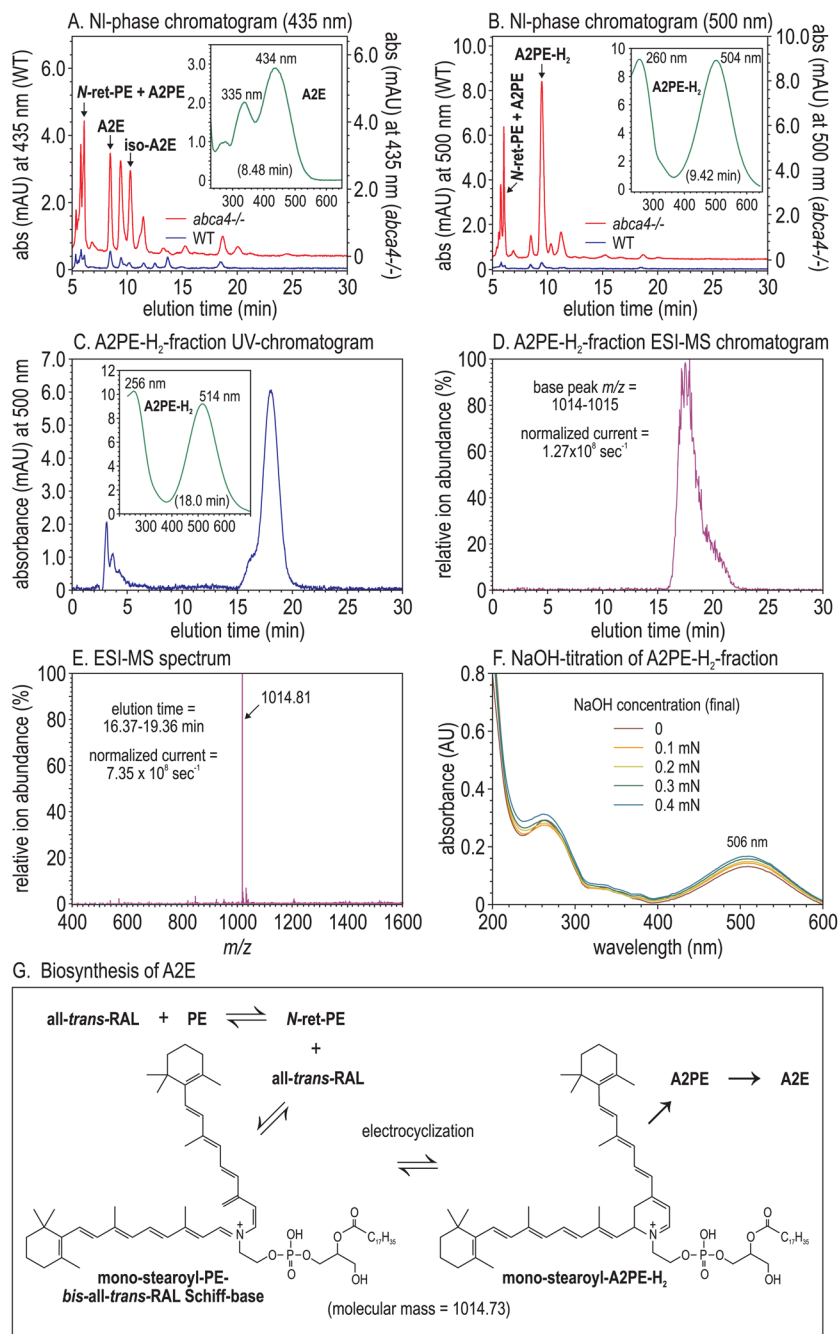


**Figure 2.** Liquid-chromatographic and mass-spectrometric analysis of A2PE-H<sub>2</sub>. **(A)** Normal-phase chromatograms at 435 nm eyecup-homogenate extracts from 8-month-old wild-type (*blue*) and *abca4*<sup>-/-</sup> (*red*) mice. A2E and iso-A2E peaks are labeled. *Inset*: UV spectrum of the A2E peak. **(B)** Normal-phase chromatograms at 500 nm of the same samples as in **(A)**. The *abca4*<sup>-/-</sup>-dependent 500-nm peak is labeled A2PE-H<sub>2</sub>. *Inset*: UV spectrum of the A2PE-H<sub>2</sub> peak. **(C)** Reverse-phase chromatogram at 500 nm of the A2PE-H<sub>2</sub> peak-fraction (9.42 minutes) collected during normal-phase chromatography of *abca4*<sup>-/-</sup> eyecup homogenates **(B)**. *Inset*: UV spectrum of the 18-minute (A2PE-H<sub>2</sub>) peak. **(D)** ESI-MS chromatogram of the sample in **(C)** showing the relative abundance of positive ions with 1014 to 1015 *m/z*. The ion current at

100% is  $1.27 \times 10^8/s$ . **(E)** MS showing the relative abundance of ions detected during the 16.37- to 19.36-minute elution interval. The ion current at 100% is  $7.35 \times 10^8/s$ . Note the near homogeneity of the 1014.81 ion. **(F)** Spectra of the A2PE-H<sub>2</sub> peak fraction from **(B)** acquired after the addition of the indicated (final) concentrations of NaOH. **(G)** Molecular structure of mono-stearoyl-A2PE-H<sub>2</sub> in equilibrium with the open-ring isomer (mono-stearoyl-phosphatidylethanolamine-*bis*-all-*trans*-RAL Schiff base).

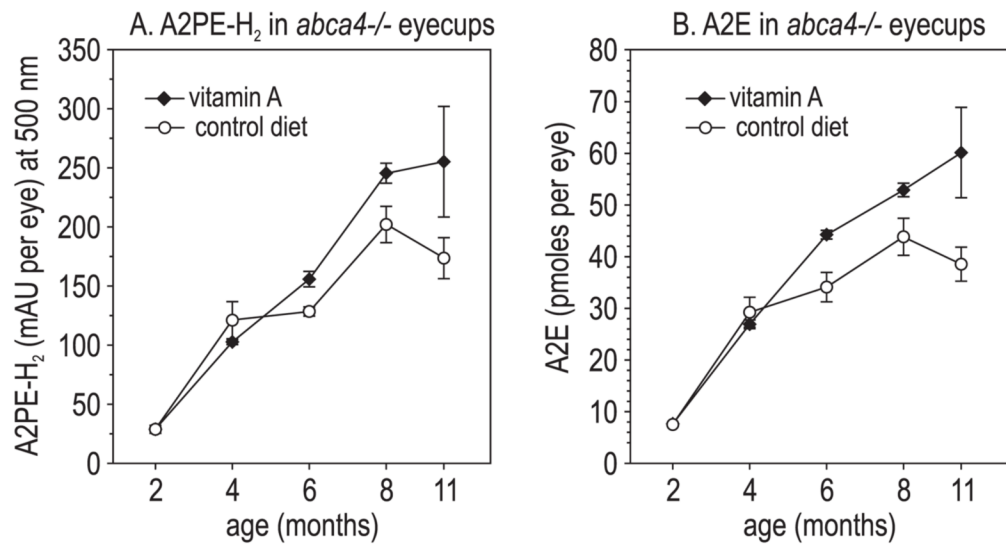


**Figure 3.** Lipofuscin fluorophores in vitamin A–treated and control-fed *abca4*<sup>-/-</sup> mouse eyes. **(A)** A2PE-H<sub>2</sub> expressed as milliabsorbance units (mAU) per eye in mice of the indicated ages. **(B)** A2E expressed as picomoles per eye. All values are shown  $\pm$ SD ( $n = 3$ ).

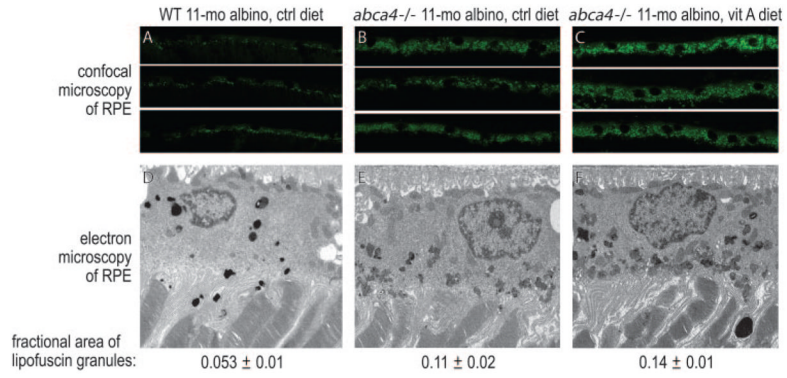


**Figure 4.** Morphologic analysis of retinas from 11-month-old albino wild-type (WT) mice on the control diet, *abca4*<sup>-/-</sup> mice on the control diet, and *abca4*<sup>-/-</sup> mice on the vitamin A (vit A)–supplemented diet. (A–C) Laser confocal images of RPE from the indicated mice showing lipofuscin autofluorescence. (D–F) Electron microscopic images of RPE cells from the indicated mice. Lipofuscin pigment granules are the small, irregularly shaped electron-dense bodies in the RPE cytoplasm. The areas (±SD) of lipofuscin pigment granules divided by total cytoplasmic areas are shown below the electron micrographs. Lipofuscin granules in the wild-type RPE section appear darker because of more intense staining with osmium salts.



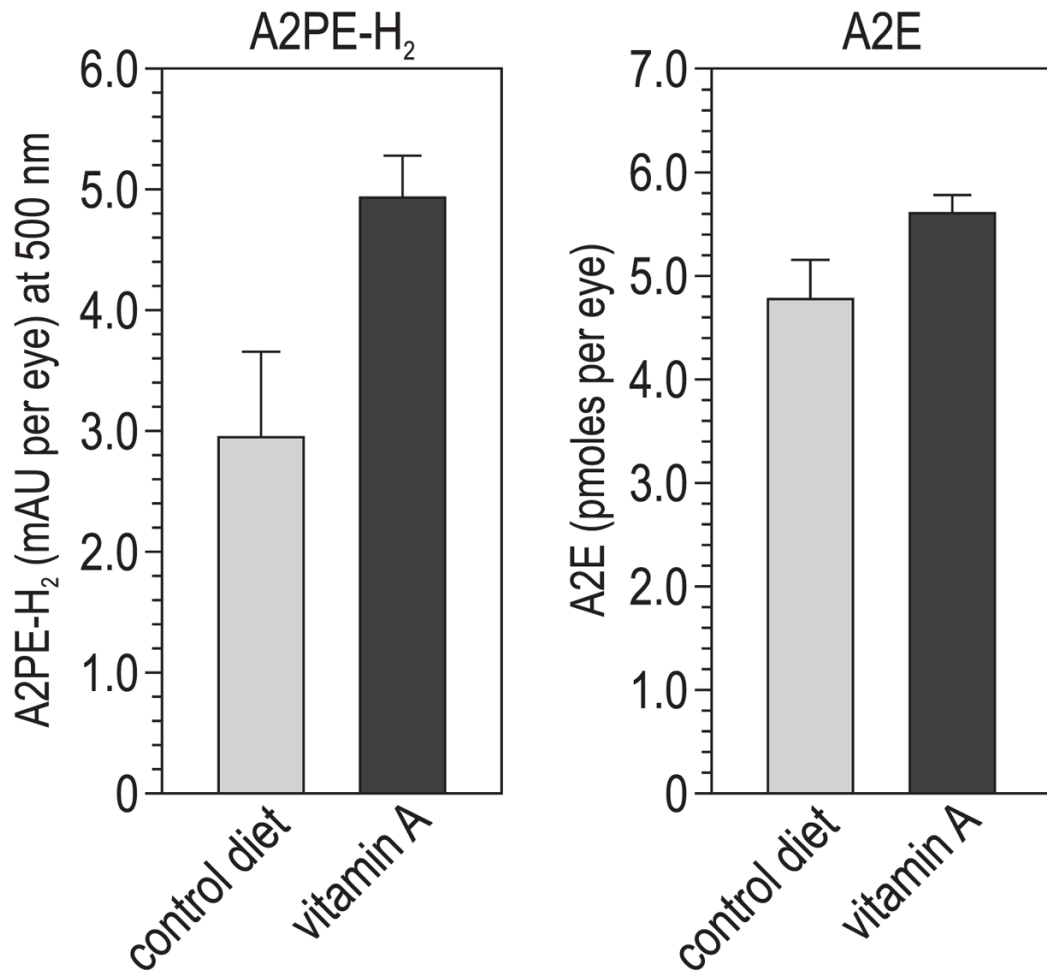


**Figure 5.** Lipofuscin fluorophores in 6-month-old wild-type (129/Sv) mice on the control or vitamin A-supplemented diet. A2PE-H<sub>2</sub> levels are shown in milliabsorbance units (mAU) per eye at 500 nm. A2E levels are shown in picomoles per eye. All values are shown  $\pm$ SD ( $n = 3$ ).

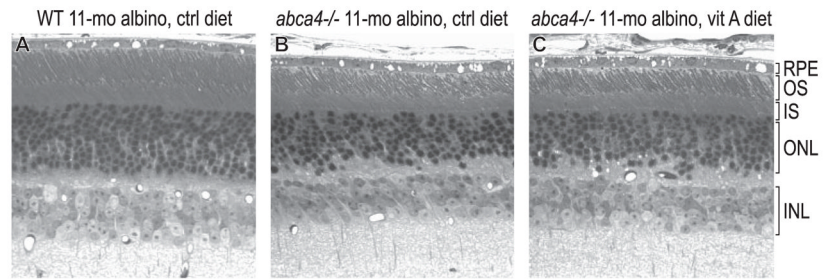


**Figure 6.**

Light micrographs of retinas from 11-month-old albino mice. (A) Wild-type mouse. (B) *abca4*<sup>-/-</sup> mouse fed the control diet. (C) *abca4*<sup>-/-</sup> mouse fed the vitamin A-supplemented diet. IS, inner segment; INL, inner nuclear layer; ONL, outer nuclear layer. Note the reduced ONL and OS thicknesses in *abca4*<sup>-/-</sup> mice, indicating partial photoreceptor degeneration and OS shortening.

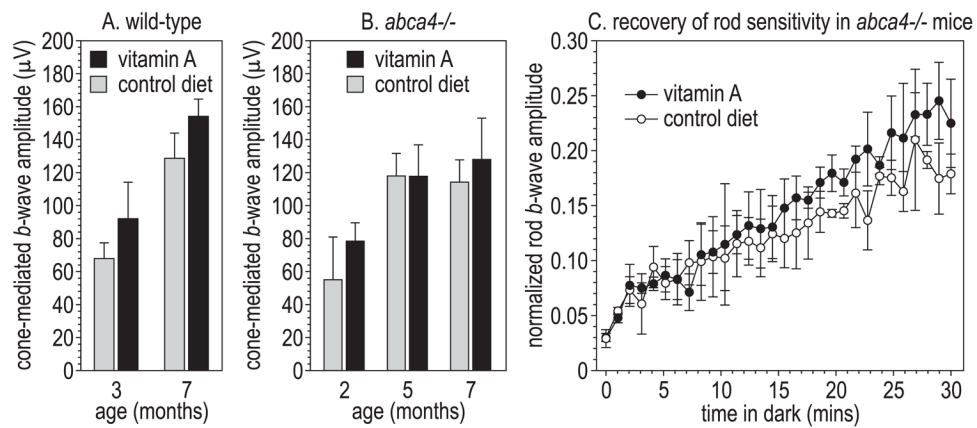


**Figure 7.**

Electroretinographic analysis. **(A)** Cone-mediated *b*-wave amplitudes in wild-type (129/Sv) mice of the indicated ages on the control or vitamin A-supplemented diet ( $n = 3-4$ ). **(B)** Cone-mediated *b*-waves in pigmented *abca4*<sup>-/-</sup> mice on control or vitamin A-supplemented diets ( $n = 4-6$ ). **(C)** Rod-mediated *b*-wave amplitudes as a fraction of the dark-adapted rod *b*-wave amplitude at the indicated times in the dark after exposure of 8-month-old *abca4*<sup>-/-</sup> mice to a light that bleached approximately 90% of the rhodopsin. All values are shown  $\pm$ SE ( $n = 3$ ).